The 2010 IEEE/RSJ International Conference on
Intelligent Robots and Systems
October 18-22, 2010, Taipei, Taiwan

Analysis of Task Feasibility for a Home Robot using Prismatic Joints

Tomoaki Mashimo, Rosen Diankov, Takateru Urakubo and Takeo Kanade.

Abstract— **This paper evaluates the dynamic and kinematic properties of a prismatic mechanism and shows its capabilities in performing home manipulation tasks when integrated into a robotic arm. Our design is motivated from the observation that human hand motions often follow a linear trajectory when manipulating everyday objects. We present the mechanical design for a light-weight, energy-efficient robot named PRISM that emphasizes translational motion. By simulating the dynamics equations and comparing the structure of commonly used anthropomorphic arms and our proposed arm, we verify that translational motion is more energy efficient with PRISM, and the robot can maneuver itself in narrower places. Through simulation experiments using state of the art manipulation planning algorithms, we analyze the success rates of PRISM and an anthropomorphic robot arm in performing basic tasks. The simulation experiments center on pick-and-place tasks in cluttered kitchen scenes. We show a real-world prototype of PRISM and perform several manipulation experiments with it.**

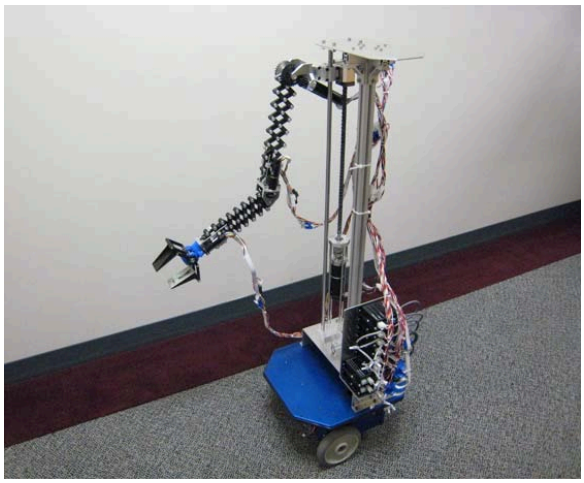

Fig. 1. Prototype of proposed robot using prismatic joints.

I. INTRODUCTION

One key technology in a robotics system designed to help elderly and handicapped people is the capability of manipulating objects around the environment [1], [2]. Successful manipulation requires both a mechanical design that is non-intrusive and a motion planning system that can handle the complexities of environment obstacles and perception error. Because most mechanical arm designs today attempt to mimic the structure of the human arm with seven rotational joints taking the roles of shoulder, elbow, and wrist [3]–[11], the mechanical design space of arms is still largely unexplored. Several robot designs employ springs and unique mechanisms to make the arms safer [12]–[16], but the kinematic structure largely remains the same. Many studies have shown that humans tend to think about grabbing objects in a hand-centric coordinate system, which implies that reaching motion also optimizes the distance the hand travels through the environment. Considering this observation along with motion capture experiments on people performing reaching tasks [17], we see that the hand roughly follows a linear trajectory to the target object roughly optimizing distance traveled in the workspace. Instead of designing a robot arm with an anthropomorphic structure as the first priority, we motivate the importance of translational motion in pick-and-place tasks and design a robot arm that prioritizes translation (Fig. 1). Compared to popular anthropomorphic arms like the Barrett WAM, we show that our design is more energy efficient, lightweight, and maneuverable when performing tasks requiring translational movement. In order to prove higher energy efficiency than anthropomorphic arms, we simulate the dynamics equations based on a simple two link example. To demonstrate maneuverability, we create kinematics model of the robots and solve for their inverse kinematics equations. Then we prepare cluttered environments of a home scenario and show that PRISM is capable of reaching its target objects a larger percentage of the time than the Barrett WAM.

One of the advantages of PRISM is its ability to freely move the elbow joint to avoid obstacles (Fig. 3). In order for anthropomorphic arms to achieve translational motion, the elbow usually has to move to adjust the distance between the shoulder and the wrist. Because the swept volume of such movements is large, a relatively large open region is required for successful motion planning (Fig. 4). PRISM employs a multi-parallel link for the prismatic mechanism, which has advantages of efficient translational motion and small swept volume. Coupled with its small non-intrusive structure, PRISM can reach very narrow places (Fig. 2).

The paper first begins with an explanation of the mechanical design of PRISM and the decisions involved in choosing the masses, lengths, and joints of the robot. We then evaluate the energy efficiency of the prismatic portion of the robot as the end-effector performs translational movements. Finally, we analyze the kinematic reachability of the robot and compare it with the Barrett WAM. We show several examples of motion planning with the robot and show the real robot executing them.

Tomoaki Mashimo, Rosen Diankov and Takeo Kanade are with the Robotics Institute at Carnegie Mellon University, Pittsburgh, PA 15213 USA (corresponding author to provide phone: 412-268-1859; fax: 412-268-6436 tmashimo@ cs.cmu.edu)

Takateru Urakubo is with Department of Computer Science and Systems Engineering at Kobe University, Kobe, 657-8501 Japan.

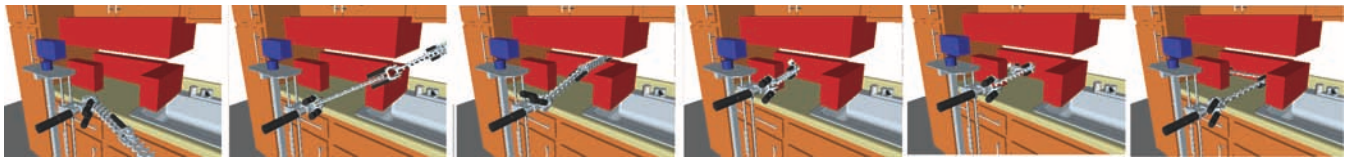

Fig. 2. Shows an automatically computed motion plan to put the arm in a narrow PRISM.

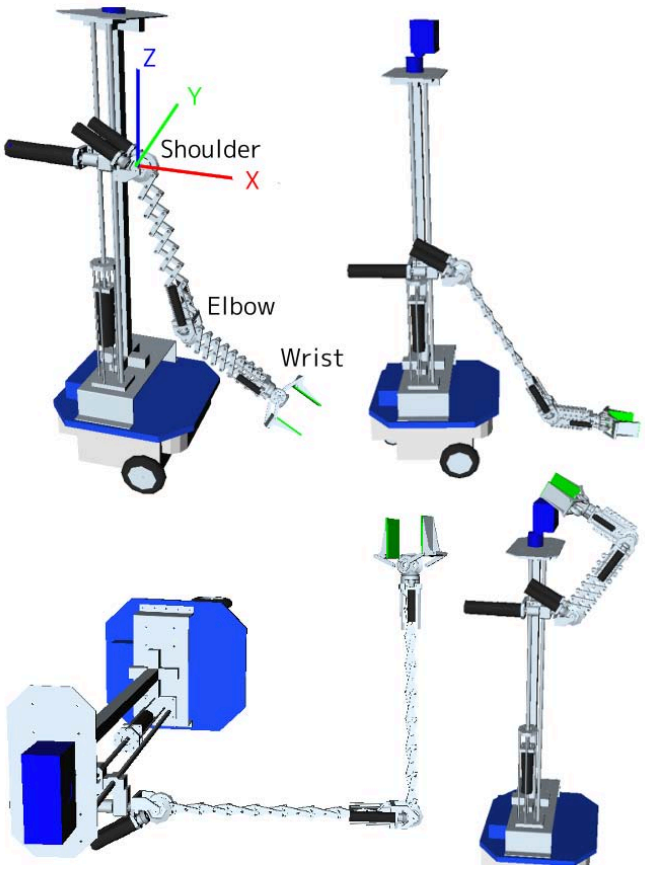

Fig. 3. The kinematics capabilities of the prismatic joints and several configurations of the robot that demonstrates ability to pick up objects from floor and reaching tasks.

II. Mechanical Design

A. Target Specifications

We define the degrees of freedom of the arm from the necessary movement for daily tasks such as object fetching. Examples of the degrees of freedom for the robot arm are shown in Table I. Most tasks can be conducted by the combination of these DOF. For example, object fetching task from floor in house is combination of retrieving motion in x-axial direction and lifting up motion in z-axial direction to a desired height. Based on the observation that a human arm roughly follows a linear trajectory [17], we design a prismatic mechanism in the the forearm and upper arm of the robot.

The relation between payload and weight is tradeoff. The mechanism using wire or belt reduces the inertia of the elbow or wrist, but the whole robot arm is heavy. In the

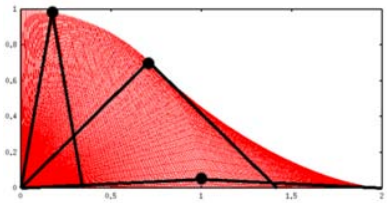

Fig. 4. The swept volume of a two link robot as it extentds is big and can limit the robots motion in the presence of many obstacles.

prismatic joint, the whole weight is reduced allowing an arm to achieve practical speed and safety. A lightweight carbon reinforced fiber plastic (CRFP) is used to show the feasibility in a prototype. The reach of the prismatic arm is approximately 1.1 meters. The length is sufficient to pick up objects into a place where handicapped and elderly people would have a difficult time to extend their arms. If reasonably mounted to a wheelchair, the arm could extend to the back of common refrigerators, microwaves or shelves. The current target payload is 1.5 kg in case the prismatic arm is completely extended, which is computed by a stress analysis using finite element method in CAD model (Pro/Engineer Mechanism, PTC co., USA). Such a payload would be sufficient for daily objects. Because payloads are dependent on the configuration of the robot, larger than 1.5 kg payloads are possible, but then motion planners would be necessary to control the arm in order to guarantee the constraints are maintained.

We prioritize the the lightweight design of wrist for the fetching objects task. The wrist has only one degree of freedom, but it allows us to reduce the weight at the end-effector further. Let us define the x, y, and z axes as in Fig. 3. The x coordinate axis is taken the horizontal extending direction of the prismatic arm. The origin is taken center of shoulder joint. In the present prismatic arm, the wrist equips only one rotation around x-axis, after two rotational DOF are removed from the wrist.

Because PRISM is capable exploiting the prismatic redundancy at the elbow, it can more easily avoid obstacles and fit into narrow places. The specification compared to the Barrett WAM is shown in Table II. The total weight of the prismatic arm is 12 kg, which is relatively practical for home environments.

B. Prismatic Mechanism

There are several ways to achieve a prismatic mechanism: screw, rack and pinion gear, electromagnetic linear motors, pneumatic actuator, and hydraulic actuator. Because driving axis of these mechanism is stiff, and the translation causes

TABLE I

DEGREES OF FREEDOM OF ROBOTS IN DAILY MOTIONS

Degrees of freedom	Example tasks
Rotation around x or y axis	Turning door knob
Rotation around z axis	Opening juice bottle
Translation in x-axial direction	Retrieving object
Translation in x and y-axial directions	Opening door
Translation in z-axial direction	Lifting up object

TABLE II

THE SPECIFICATION OF THE PRISMATIC ROBOT ARM

Position	Range
Vertical translation of the manipulator	0.5 m
Rotation around x axis at shoulder	π rad (180 $^\circ$)
Rotation around y axis at shoulder	π rad (180 $^\circ$)
Translation of upper arm	0.37 m
Rotation around y axis at elbow	π rad (180 $^\circ$)
Translation of forearm	0.37 m
Rotation around x axis at wrist	2π rad (360 $^\circ$)
Translation of gripper	80 mm

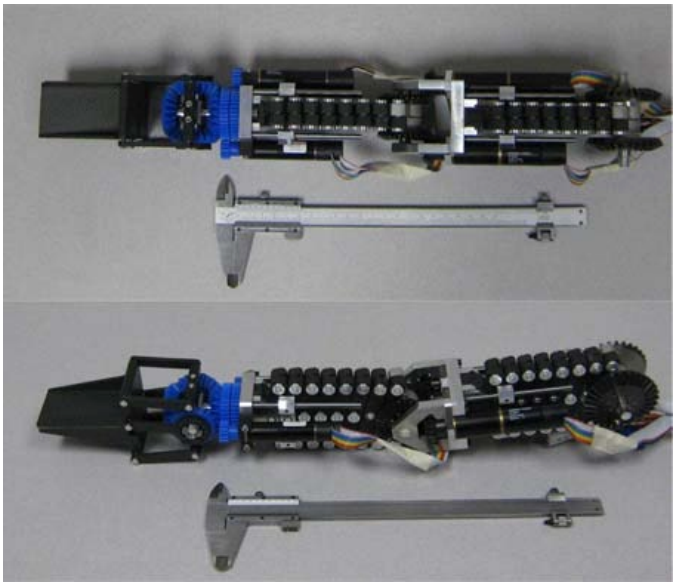

Fig. 5. Prismatic robot arm with differential drive that makes revolute and prismatic motions

the danger that the driving axis hits human. Several research group considered a prismatic joint for flexibility of the manipulator in the past [18]–[21]; however, most of the experiments were in simulation. To realize a mechanism with expansion and contraction for avoiding danger, we employ a multi-parallel link[1] [22], [23]. To our knowledge, efficient dynamic characteristics of the multi parallel link have not exploited. Compared with humanlike robot arms, the prismatic arm with multi-parallel link shows better efficiency at least as long as the wrist follows straight trajectory. The multi-parallel link composed of 36 links (16 rhombus) is given as shown in Fig. 3.

C. Prototype

The prismatic arm is composed of multi-parallel links and differential drive that generates prismatic and/or revolute DOF. The mechanism achieves a compact joint as shown in Fig. 5. In general, the mechanism using differential gear has two rotational DOF and enlarges the joint. The motion of the prismatic arm is dependent on the relative motion of the two gears. If the gears move in the same direction, the mechanism revolves around the axis. If the gears move in opposite directions, the mechanism moves linearly. By adjusting the relative motion, it is possible to generate a movement that moves both rotationally and linearly. The differential gear is efficient to realize two DOF with high energy density required for robots. The differential drive mechanism with multi-link is attached to the shoulder and elbow. Wrist employs a differential gear for gripping an object and rotating itself. In addition, the prismatic arm has actuators for the horizontal rotation at the shoulder and for a vertical translation. Accordingly, the prismatic arm has four revolute DOF, three prismatic DOF, and 1 gripping DOF. The gripper moves the both finger in parallel direction. All DOF of the prismatic arm is shown in Table III. The prismatic arm equips the necessary DOF to work in human environment. The prismatic arm has the peak revolution of 6.28 rad/s at each joint and the peak translation of 500 mm/s at the forearm, close to the speed of human's daily motion. The peak revolute and prismatic speeds are defined by performances of electromagnetic motors. The prismatic arm aims to lift and holding objects of 1.5 kg at best when the arm is extended horizontally. Based on the concept of lightweight and safe, we designed to lighten the prismatic arm. The ideas for lighting weight are: (1) The wrist is light because it has 1 rotational DOF. (2) The prismatic arm employes the differential drive with prismatic and revolute motions at elbow and wrist. (3) The links in the prismatic arm are made of a CRFP with lightweight and strong. The material is expensive, but the simple structure of the link might make the fabrication easy.

TABLE III

MOVABLE RANGE AND SPECIFICATION OF THE PRISMATIC ROBOT ARM

Specification	WAM arm	New arm
Reach	1 m	1 m
Degrees of freedom	7	7
Torso	0	1 (Linear)
Shoulder	3	3 (1 linear)
Elbow	1	2 (1 linear)
Wrist	3	1
Weigh beyond shoulder	5.8 kg	2. kg
Total weight	27 kg	13 kg

[1]This mechanism is occasionally called *lazy tong* or *scissors jack*

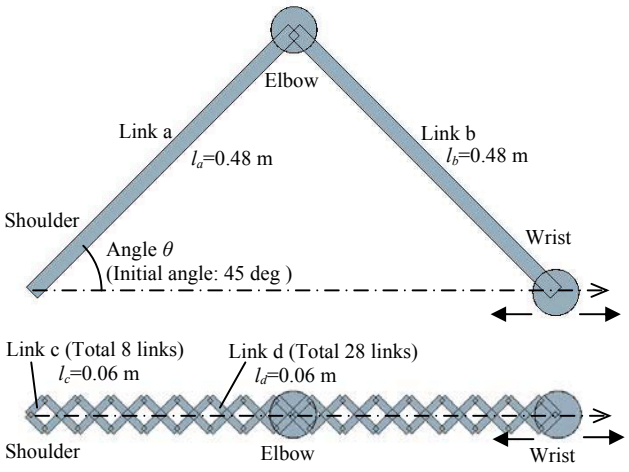

Fig. 6. Schematic of the dynamics computation

TABLE IV
MODEL PARAMETERS FOR THE SIMULATION

	Weight [kg]	MoI * [kgm^2]	Total weight [kg]
Link a	0.268	5.16×10^{-3}	-
Link b	0.268	5.16×10^{-3}	-
Elbow	0.474	0.248×10^{-3}	-
Wrist	0.474	0.248×10^{-3}	-
Link c (Total 8 links)	0.0084	0.698×10^{-6}	0.0672
Link d (Total 28 links)	0.0168	5.17×10^{-6}	0.470

*) MoI (moment of inertia) is around the center of mass

III. DYNAMIC SIMULATION

The dynamic performance of the prismatic arm with multi-parallel links model (Multi-link model) is compared to a model of anthropomorphic arm with two bar linkages model (Two-link model). The both models are shown in Fig. 6 and the mass properties of the both model are shown table IV. The both models have same mass properties in those different structures for the fair comparison calculation. The total weight of 36 links in the multi-link model is equal to the total weight of two link arm. In the simulation, two virtual weights are attached at the wrist and elbow instead of a joint mechanism. Gravity and friction are ingnored to evaluate the horizontal motions of the arm. When a linear trajectory is given to the model, the necessary torque is calculated by inverse dynamics. The desired position θ_d at the joint is given as an input

$$\theta_d = A\sin(\omega t + \theta_0) \ , \tag{1}$$

where A is amplitude, ω is angular velocity, t is time, and θ_0 is initial angle. The wrist is defined to move on the straight on x-axial direction. The position of the wrist is expressed as

$$x = (n-1)l\cos\theta \tag{2}$$

where n is number of links, l is the length of the link. In the inverse dynamics computation, The initial angle of the models is 45° at 0 s. The models are extended at 1 s and return to the initial angle at 2 s. They are contracted at 3 s and return again at 4 s. Fig. 7 show the result of the computation. In the both models, the torques are low when the arm is extended, and they are high when the arm is contracted as well as a mechanism of slider-clank.

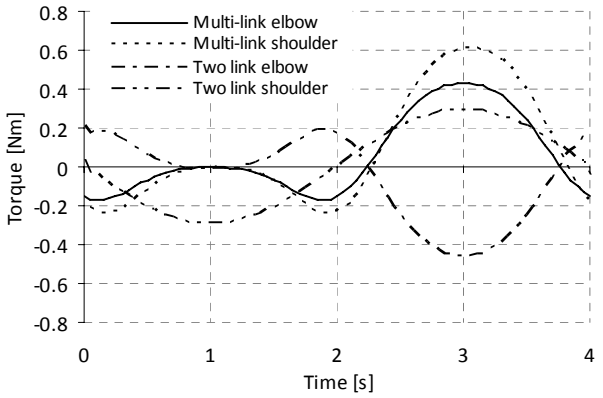

Fig. 7. Torque of each joint of multi-link and two link

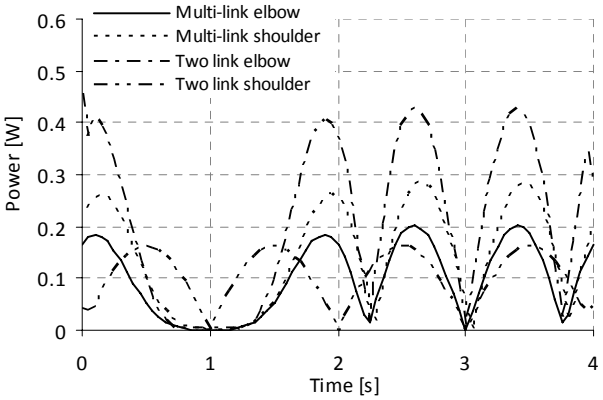

Fig. 8. Work of each joint of multi-link and two link

Compared to the two-link model, the multi-link model can be moved by relatively small torque at the range that the multi-link model is extended. By this characteristic, the prismatic arm can generate impulsive force as long as the prismatic arm reaches over. This impulsive force is effective for the case that a robot arm pulls to open the door knob or the handle of drawer or lift up heavy objects from floor.

Fig. 8 shows the power of the actuator required at the elbow and shoulder in two-link model and multi-link model. In the multi-link model, the difference of the power between its elbow and shoulder is approximately 1.5 times. The elbow in two-link model needs largest power for the movement. The reason for the large power is that the revolution of the elbow joint is twice than that of the shoulder. This result indicates that a robot arm such the two-link model requires high power for the drive. If the power source cannot generate the enough power, the revolution be decreased. It causes a decrease of the motion speed of the robot arm.

Fig. 9 shows the mechanical energy for the both motions.

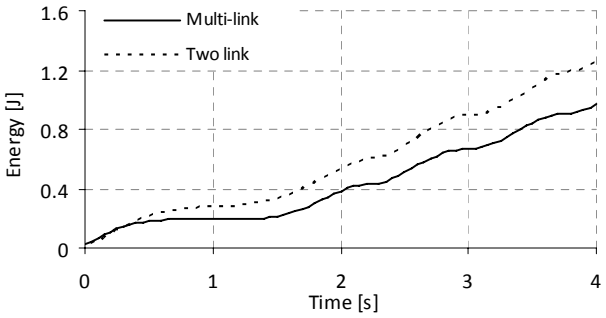

Fig. 9. Mechanical energy of multi-link and two link (lower is better).

The energy of the multi-link model achieved approximately 25 % efficient than that of the two-link model. It is mainly due to the moment of inertia of whole links and the joint weight at elbow. Because the each link in multi-link model is short and rotates around its center of mass, the moment of inertia is low.

IV. Task Performance and Execution

Evaluating a robot on how well its kinematics are suited to autonomously perform manipulation tasks requires the combination of object grasping analysis, motion planning algorithms, and inverse kinematics calculations. A quick look at PRISM's reachability density (Fig. 10) shows that it can grasp objects up to 1.1 meters away from its base axis of rotation. Because the arm concentrates on translation motion more than rotation, the density quickly falls off suggesting that not many rotations are possible further away. The measure we choose to evaluate a robot is based on the capability that it can successfully pick up an object given a random environment in simulation. These types of manipulation problems are usually decomposed into finding the grasp locations for the object, finding the robot configuration to satisfy the grasps, and then searching for a feasible trajectory that connects the initial robot configuration to the goal configuration while avoiding obstacles [24]. In order to simplify development, we use OpenRAVE [25] for the manipulation and grasp planning algorithms.

We build a grasp set for each target object by simulating the approach of the gripper to the target object from all possible directions. After the gripper gets close to the object, we compute the contact points it makes; if the target object is in force closure, we store the grasp with respect to the target object coordinate system (Fig. 11).

Given a target object, we use the grasp sets to compute possible grasps that are collision-free of the environment and are guaranteed to stably grasp the object. Because the search space for robot arms is seven dimensions, it is very time consuming to sample random robot configurations until they approach the goal. Instead, most researchers first compute the robot configurations that can reach the grasps using inverse kinematics algorithms. There exist a multitude of numeric IK solvers, but they have the disadvantage of long computation

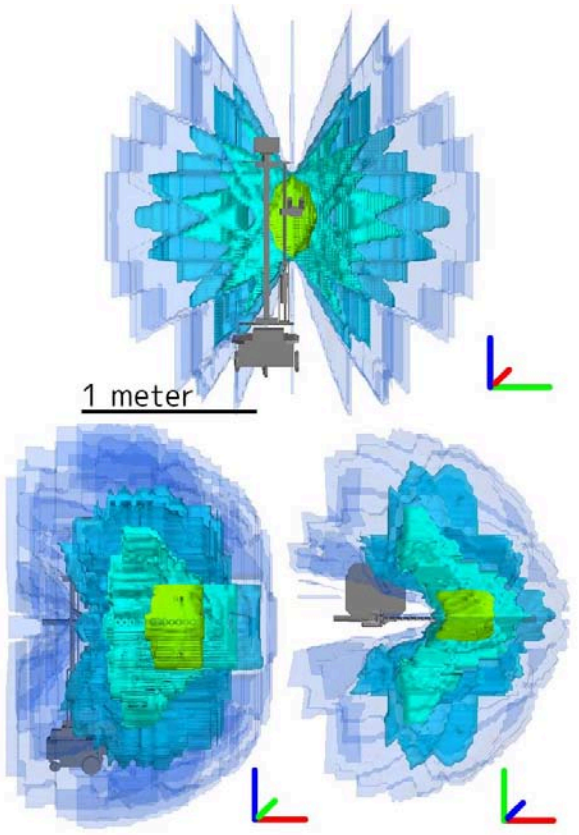

Fig. 10. The reachability area density of the gripper considering self-collisions (hotter areas have higher density).

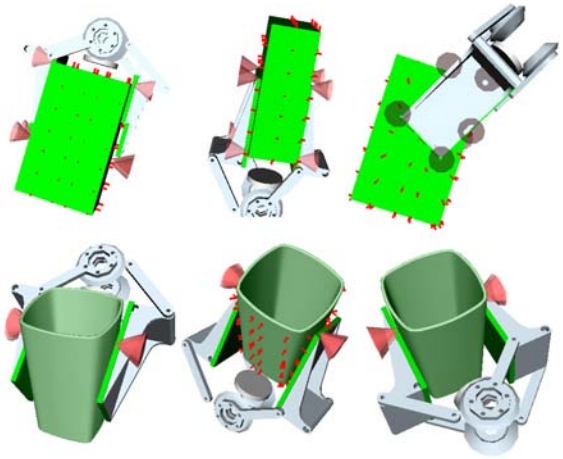

Fig. 11. Some of the automatically generated grasps used in the task evaluation experiments.

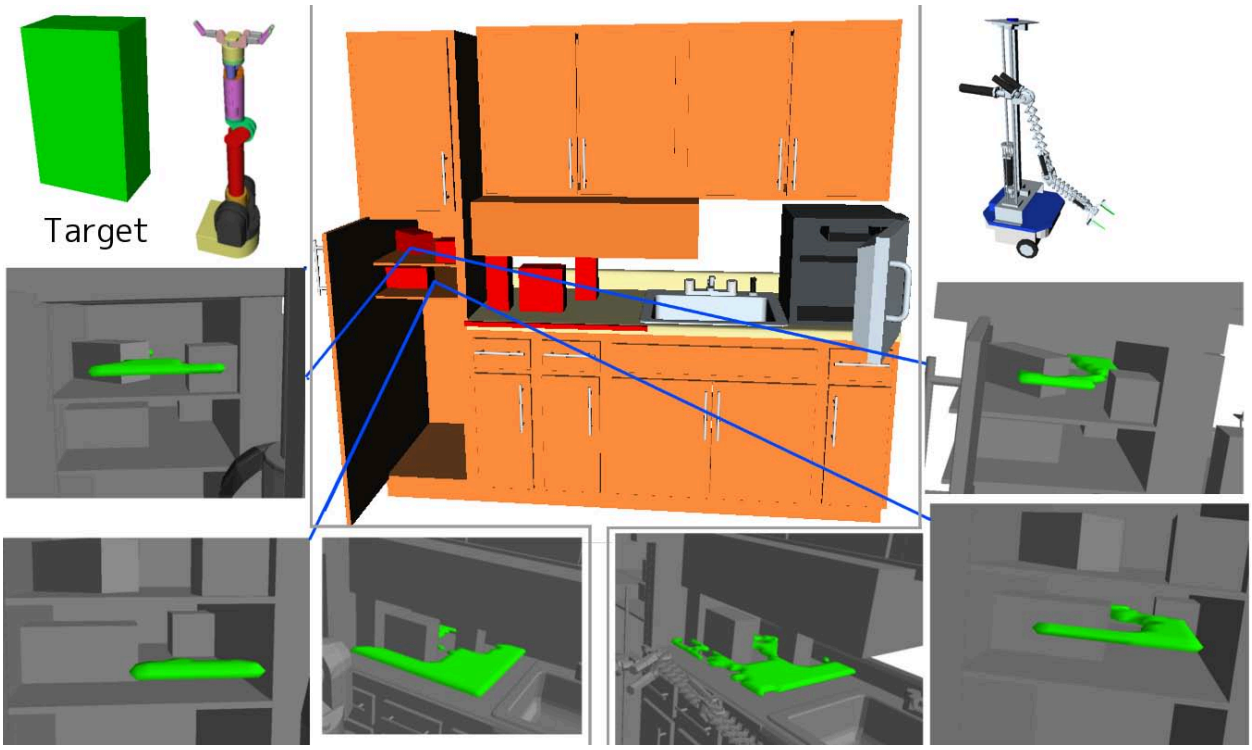

Fig. 12. Three different sections of this kitchen scene were used to test the locations in which the target object can be safely grasped without colliding. The left side shows the *graspability region* for the WAM while the right side shows the *graspability region* for PRISM.

times and do not give all possible solutions, therefore we analytically solve the closed-form inverse kinematics equations of PRISM using the help of OpenRAVE's **ikfast**. PRISM has seven joints: three prismatic and four rotational. Because the gripper pose is six dimensions, we first take the elbow joint as a *free parameter* and are left with six joints that we can fully solve for. Because the translational joints do not affect the rotation of the gripper in anyway, we can separate solving for the rotation and the translation: we first solve for the rotational joints using standard methods, then we solve for the translational joints. The kinematics had many degenerate cases, so the generated analytical IK solver became 100,000 lines of C++ code, which is 20 times larger than Barrett WAM's. Even so, the execution time is on the order of 50 microseconds. Once the goal robot configurations are computed, we use Bi-directional RRTs [26] to find a collision-free trajectory.

Because the advantages of PRISM over other robots is its slender arm and capability to translate without moving its elbow, we choose particularly narrow scenes when comparing it with the Barrett WAM (Fig. 12). We first pick a region in the environment and center the robot around it. Then for every 2D point on the surface, we test if a target object at any orientation can be picked up from that location, we call all possible locations the *graspability region*. Table V shows the percentage of the regions computed for Fig. 12 for the target object shown. On cluttered scenes, PRISM is able to outperform the WAM since it can reach tighter places, but on open scenes where there aren't as many obstacles, the WAM has a higher *graspability* region.

TABLE V
GRASPABILITY REGION

	WAM	PRISM	Region Ratio
Table Surface	**53.2%**	50.0	0.94
Lower Shelf	8.5%	**26%**	3.05
Upper Shelf	17.2%	**31.2%**	1.81

A. Real-world Experiments

In order to build PRISM (Fig. 13), we used Maxon motors with the EPOS controller interface. The controller loop was a 250Hz PID loop on linearly interpolated trajectories coming from the planning system. Current the biggest problem with the implementation is that the multi-link prismatic joints have a tendency to deform slightly as trajejectories are executed, this sometimes causes the robot to collide with obstacles when it shouldn't. In the future, we will make the mechanism stronger to account for this problem.

V. CONCLUSION

In this paper we proposed a novel robotic arm and analyzed its dynamics and kinematics properties in the context of executing daily pick-and-place tasks. Because of the lightweight nature of the robot, achieving a sturdy prismatic joint that does not deflect due to forces is difficult.

ACKNOLWEDGEMENTS

This research has been supported in part by the National Science Foundation's Quality of Life Technology Center.

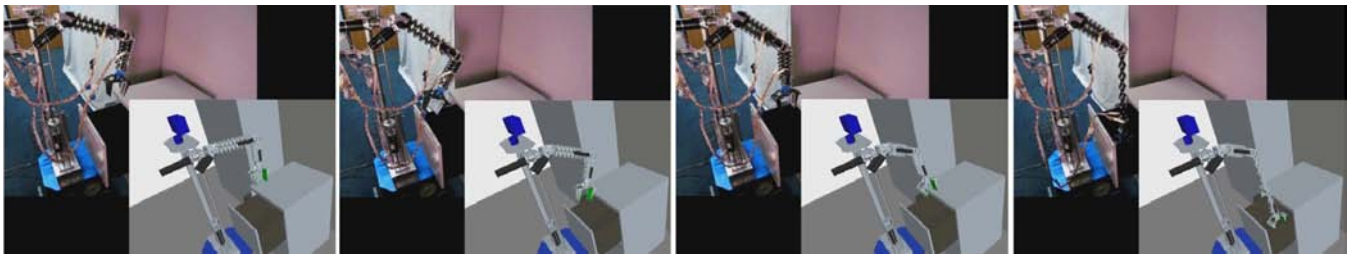

Fig. 13. Video of the real robot synchronized with the OpenRAVE world and reaching into a drawer.

REFERENCES

[1] C. A. Stanger, C. Anglin, W. S. Harwin, and D. P. Romilly, "Devices for assisting manipulation: a summary of user task priorities," IEEE Transactions on Rehabilitation Engineering, vol. 2, no. 4, pp. 256-265, 1994.

[2] C. K. Charles, D. A. Cressel, N. Hai, J. T. Alexander, and X. Zhe, "A point-and-click interface for the real world: laser designation of objects for mobile manipulation," in Proc. 3rd ACM/IEEE international conference on Human robot interaction Amsterdam, The Netherlands: ACM, 2008.

[3] K. Salisbury, W. Townsend, B. Ebrman, and D. DiPietro, "Preliminary design of a whole-arm manipulation system (WAMS)," in Proc. 1988 IEEE International Conference on Robotics and Automation, 1988, pp. 254-260 vol.1.

[4] K. Hirai, M. Hirose, Y. Haikawa, and T. Takenaka, "The development of Honda humanoid robot," in Proc. 1998 IEEE International Conference onRobotics and Automation, 1998, pp. 1321-1326 vol.2.

[5] K. Nishiwaki, T. Sugihara, S. Kagami, F. Kanehiro, M. Inaba, and H. Inoue, "Design and development of research platform for perception-action integration in humanoid robot: H6," in Proc. 2000 IEEE/RSJ International Conference on Intelligent Robots and Systems, 2000, pp. 1559-1564 vol.3.

[6] B. Driessen, H. Evers, and J. v Woerden, "MANUS-a wheelchair-mounted rehabilitation robot," Proceedings of the Institution of Mechanical Engineers, Part H: Journal of Engineering in Medicine, vol. 215, no. 3, pp. 285-290, 2001.

[7] R. Brooks, L. Aryananda, A. Edsinger, P. Fitzpatrick, C. C. Kemp, U.-M. O'Reilly, E. Torres-Jara, P. Varshavskaya, and J. Weber, "Sensing and Manipulating Built-for-human Environments," International Journal of Humanoid Robotics, vol. 1, no. 1, pp. 1-28, 2004.

[8] K. Kaneko, F. Kanehiro, S. Kajita, H. Hirukawa, T. Kawasaki, M. Hirata, K. Akachi, and T. Isozumi, "Humanoid robot HRP-2," in Proc. 2004 IEEE International Conference onRobotics and Automation, 2004, pp. 1083-1090 Vol.2.

[9] P. Ill-Woo, K. Jung-Yup, L. Jungho, and O. Jun-Ho, "Mechanical design of humanoid robot platform KHR-3 (KAIST Humanoid Robot 3: HUBO)," in Proc. 5th IEEE-RAS International Conference on Humanoid Robots, 2005, pp. 321-326.

[10] T. Asfour, K. Regenstein, P. Azad, J. Schroder, A. Bierbaum, N. Vahrenkamp, and R. Dillmann, "ARMAR-III: An Integrated Humanoid Platform for Sensory-Motor Control," in Proc. 6th IEEE-RAS International Conference on Humanoid Robots, 2006, pp. 169-175.

[11] P. Deegan, R. Grupen, A. Hanson, E. Horrell, S. Ou, E. Riseman, S. Sen, B. Thibodeau, A. Williams, and D. Xie, "Mobile manipulators for assisted living in residential settings," Autonomous Robots, vol. 24, no. 2, pp. 179-192, 2008.

[12] G. Hirzinger, A. Albu-Schaffer, M. Hahnle, I. Schaefer, and N. Sporer, "On a new generation of torque controlled light-weight robots," in Proc. 2001 IEEE International Conference on Robotics and Automation, 2001, pp. 3356-3363 vol.4.

[13] A. Bicchi and G. Tonietti, "Fast and "soft-arm" tactics [robot arm design]," IEEE Robotics and Automation Magazine, vol. 11, no. 2, pp. 22-33, 2004.

[14] K. A. Wyrobek, E. H. Berger, H. F. M. Van der Loos, and J. K. Salisbury, "Towards a personal robotics development platform: Rationale and design of an intrinsically safe personal robot," in Proc. 2008 IEEE International Conference on Robotics and Automation, 2008, pp. 2165-2170.

[15] M. Zinn, O. Khatib, and B. Roth, "A new actuation approach for human friendly robot design," in Proc. 2004 IEEE International Conference onRobotics and Automation, 2004, pp. 249-254 Vol.1.

[16] D. Shin, I. Sardellitti, Yong-Lae Park, O. Khatib, M. Cutkosky. "Design and Control of a Bio-inspired Human-Friendly Robot," in Proc. of the 11th International Symposium on Experimental Robotics, 2008.

[17] J. J. Marotta, W. P. Medendorp, and J. D. Crawford, "Kinematic Rules for Upper and Lower Arm Contributions to Grasp Orientation," J Neurophysiol, vol. 90, no. 6, pp. 3816-3827, December 1, 2003 2003.

[18] K. W. Buffinton, "Dynamics of Elastic Manipulators With Prismatic Joints," Journal of Dynamic Systems, Measurement, and Control, vol. 114, no. 1, pp. 41-49, 1992.

[19] H. Zhuang and Z. S. Roth, "A linear solution to the kinematic parameter identification of robot manipulators," IEEE Transactions on Robotics and Automation, vol. 9, no. 2, pp. 174-185, 1993.

[20] J. I. Imura, K. Kobayashi, and T. Yoshikawa, "Nonholonomic control of 3 link planar manipulator with a free joint," in Proc. of the 35th IEEE Decision and Control, 1996, pp. 1435-1436 vol.2.

[21] A. S. Deo and I. D. Walker, "Minimum effort inverse kinematics for redundant manipulators," IEEE Transactions on Robotics and Automation, vol. 13, no. 5, pp. 767-775, 1997.

[22] N. Hara, K. Tanaka, H. Ohtake, and H. O. Wang, "Development of a Flying Robot With a Pantograph-Based Variable Wing Mechanism," IEEE Transactions on Robotics, vol. 25, no. 1, pp. 79-87, 2009.

[23] Z. Xu, T. Deyle, and C. C. Kemp, "1000 Trials: An Empirically Validated End Effector that Robustly Grasps Objects from the Floor," in Proc. 2009 IEEE International Conference on Robotics and Automation, 2009, pp.100-100

[24] Rosen Diankov, Nathan Ratliff, Dave Ferguson, Siddhartha Srinivasa, James Kuffner. "BiSpace Planning: Concurrent Multi-Space Exploration." Robotics: Science and Systems Conference, June 2008.

[25] Rosen Diankov and James Kuffner. "OpenRAVE: A Planning Architecture for Autonomous Robotics," tech. report CMU-RI-TR-08-34, Robotics Institute, Carnegie Mellon University, July, 2008.

[26] J. Kuffner and S. LaValle, "RRT-Connect: An Efficient Approach to Single-Query Path Planning," in Proceedings of the IEEE International Conference on Robotics and Automation (ICRA), 2000.